Unified understanding of the electron-phonon coupling strength for nanocarbon allotropes

Shota Ono,[1,*] Yasunori Toda,[2] and Jun Onoe[3]

[1]*Department of Physics, Graduate School of Engineering,Yokohama National University, Yokohama 240-8501, Japan*

[2]*Division of Applied Physics, Faculty of Engineering, Hokkaido University, Sapporo 060-8628, Japan*

[3]*Department of Physical Science and Engineering, Nagoya University, Nagoya 464-8603, Japan*

(Received 8 April 2014; revised manuscript received 3 September 2014; published 21 October 2014)

The electron-phonon coupling constant (λ) of carbon nanotubes ($\lambda = 0.006$) is much smaller than that of alkali-metal-doped C_{60} crystals ($\lambda = 0.6$). This difference may be due to the shape of the π-electron conjugated system: the former has a flat, whereas the latter has a sphere. In order to confirm the shape effects in λ, we have examined the magnitude of λ for a one-dimensional (1D) uneven peanut-shaped C_{60} polymer that has an intermediate shape of the π-electron conjugated system between a carbon nanotube and a C_{60} system, using femtosecond (fs) time-resolved pump-probe spectroscopy, because it can be expected to have an intermediate value of λ between them. Theoretical analysis of fs-transient refractivity obtained experimentally found the magnitude of λ of the 1D C_{60} polymer film to be 0.02 as our expectation. This indicates that the shape of the π-electron conjugated system affects the magnitude of λ for nanocarbon allotropes significantly.

DOI: 10.1103/PhysRevB.90.155435 PACS number(s): 78.67.Ch, 63.20.kd, 78.40.Ri, 78.47.jp

I. INTRODUCTION

Electron-phonon (e-ph) interaction is one of the most key ingredients for understanding the electronic properties of nanocarbon allotropes, because it is related to many physical phenomena such as superconductivity [1,2], charge-density-wave (CDW) [3], electron transport [4], and optical responses [5,6]. The e-ph coupling constant λ [7] has been determined for those systems so far [8–13]: For example, $\lambda \simeq 0.6$ for A_3C_{60} [9] and $\lambda \simeq 0.1$ for A_1C_{60} [10] with A = K, Rb, Cs, while $\lambda \simeq 0.006$ for single-walled carbon nanotubes (CNTs) [12] and $\lambda \simeq 5.4 \times 10^{-4}$ for multiwalled CNTs [13].

What causes the large difference in the magnitude of λ between CNTs and C_{60} systems? When both systems are compared to each other, the former CNTs have a flat-shaped π-electron conjugated system along the electron-conductive direction, whereas the latter C_{60} have a spherically shaped π-electron one. This suggests that the shape of π-electron conjugation influences the magnitude of λ for nanocarbon allotropes. Given that C_{60} molecules were coalesced to form a structure like CNTs via the generalized Stone-Wales (GSW) rearrangement [14], we could examine the shape effects on the magnitude of λ and thus confirm the above speculation. Although it was reported that C_{60} molecules react with each other to form a polymer inside a CNT [15], it is reasonable to consider that the value of λ in the C_{60} polymer thus formed is significantly modified by the exterior tubes: The shape effects on λ are not directly observed in the systems. Fortunately, the recent discovery of a one-dimensional (1D) uneven peanut-shaped C_{60} polymer enables us to confirm the speculation described above.

The 1D C_{60} polymer has been synthesized from electron-beam (EB) irradiation of pristine C_{60} films via the GSW transformations between adjacent C_{60} molecules, as shown in Fig. 1 [16–19], thus it is expected that the shape effects on λ can be observed in such systems because of no exterior tube. The 1D C_{60} polymer has a cross-linked structure roughly close to that of the P08 C_{120} isomer (obtained via GSW) [17]. In other words, the coalescence among nC_{60} molecules gives rise to form a 1D $(C_{60})_n$ polymer (n is a positive integer). In case of $n = 2$, there has been reported to be 24 C_{120} structural isomers obtained via GSW, and one of which is equivalent to the shortest capped (5,5)CNT [20]. Because the 1D peanut-shaped C_{60} polymer has an intermediate shape of a π-electron conjugated system between (5,5)CNT and pristine solid C_{60}, it can be expected that the 1D polymer has an intermediate value between 0.006 and 0.6. In addition, the 1D C_{60} polymer exhibits fascinating phenomena such as geometrical curvature effects on Tomonaga-Luttinger liquid states [21], CDW transition at 50 K [22,23], and anomaly in the resistivity at temperatures lower than 50 K [24]. In particular, the latter two properties are also related to the e-ph interaction and thus inspire us to examine the magnitude of λ for the 1D C_{60} polymers.

In the present work we report on the λ value of the 1D uneven peanut-shaped C_{60} polymer by examining the temperature dependence of the relaxation time of photoexcited electrons in the polymer, and confirm that the shape of π-electron conjugation affects the magnitude of λ for nanocarbon allotropes.

In Sec. II we describe briefly experimental details. In Sec. III we show measured transient reflectivity changes and confirm that these results are consistent with the previously measured one [22]. From these data we estimate the e-ph coupling constant using a theoretical model. In Sec. IV we confirm that the estimated length of the 1D C_{60} polymer from the magnitude of the e-ph coupling is quite similar to the previous data obtained by the resistivity measurement [24]. We also compare the magnitude of the e-ph coupling of the 1D C_{60} polymer with that of other nanocarbon allotropes. In Sec. V we conclude our paper.

II. EXPERIMENTS

Metallic 1D uneven peanut-shaped C_{60} polymers were formed from 3-kV electron-beam irradiation of a 500-nm-thick pristine C_{60} film deposited on a cesium iodide (CsI) substrate

*shota-o@ynu.ac.jp

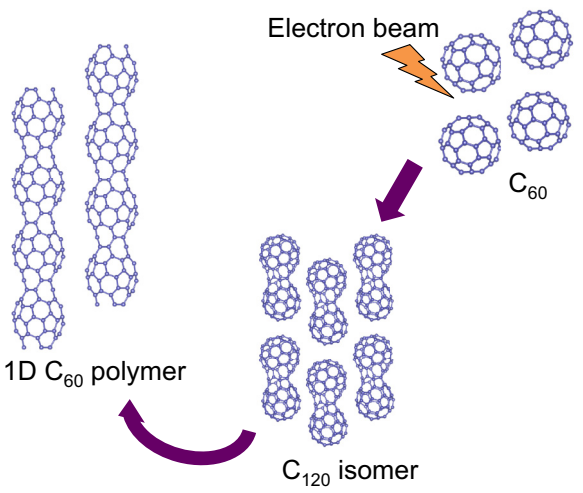

FIG. 1. (Color online) Schematic illustration showing the synthesis of the 1D C_{60} polymer. When the electron beam is irradiated to C_{60}, two C_{60} are coalesced with each other via the GSW transformation and transformed into C_{120} isomers, followed by the synthesis of the 1D C_{60} polymer.

(15 mm in diameter, 2 mm thick) for approximately 200 h in an ultrahigh vacuum (UHV) chamber (a base pressure $<10^{-6}$ Pa) equipped with a high-resolution (0.25 cm^{-1}) Fourier-transform infrared (FT-IR) spectroscopy (Mattson Research Series). The formation of the 1D C_{60} polymers was confirmed by FT-IR spectra measured *in situ* [25]. A slight blueshift of the optical phonon frequency was observed due to the bundling of the polymers [26]. In addition, the 1D structured C_{60} polymer has been confirmed using electron diffraction [27]. Furthermore, we have measured the ultraviolet-visible absorption spectra of pristine C_{60} and 1D C_{60} polymers films. The pristine C_{60} shows intense peaks at 350 nm (3.54 eV) and 450 nm (2.75 eV), corresponding to the HOMO-1 and HOMO bands, respectively, whereas the 1D C_{60} polymers film shows that the absorption bands are broadened and continuum, where the absorption edge spread over to a wavelength longer than 1100 nm (less than 1.14 eV) [29]. Similar band structures have been observed in the photoemission spectra: Some intensive narrow bands become broadened after the EB irradiation, and the valence electronic states spread toward the Fermi level, clearly indicating the absence of the energy gap [30]. Thereafter, the 1D polymer film on CsI was taken out of the UHV chamber, and mounted on a copper holder within a liquid helium flow cryostat. We used a femtosecond (fs) UV/NIR pump-probe spectroscopy to measure the relaxation time of photoexcited electrons. The light sources were generated from a mode-locked cavity-dumped Ti:sapphire laser with a repetition rate of 270 kHz, and a pulse duration of 120 fs. The UV (3.0 eV) pump pulses with a fluence of 50 mJ/cm^2 were produced by the second harmonic generation (SHG) of the laser. The nonequilibrium electron transients induced by the pump were evaluated by the reflectivity changes of the NIR (1.5 eV) probe pulses whose fluence was an order of magnitude weaker than that of the pump. The excited carriers created by the pump pulse are thermalized within a few hundred fs through the electron-electron scatterings and obey the Fermi-Dirac distribution function with an electron temperature higher than the lattice temperature [31]. These excess carriers above the Fermi level would be re-excited by absorbing the probe pulses, which leads to the transient changes in the reflectivity. Although the 1D C_{60} polymer was polycrystalline on the CsI substrate (crystalline size: 8–18 nm from XRD), the transient responses were not affected by grain boundaries but reflected the carrier relaxation dynamics peculiar to the quasi-1D structures [22].

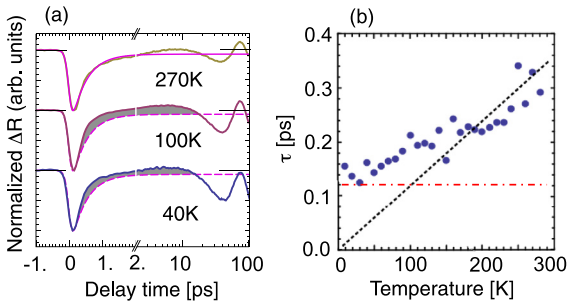

FIG. 2. (Color online) (a) The normalized reflectivity ΔR as a function of delay time t of 1D C_{60} polymers at $T = 40$, 100, and 270 K. The shaded areas (gray) indicate the differences from the fitting obtained at $T = 270$ K. The oscillations at $t > 10$ ps are due to the acoustic pulses. (b) T dependence of τ. The dashed line is the fits to the data using Eq. (2). The dashed-dotted line (red) is the pulse width of 120 fs.

III. RESULTS AND ANALYSES

A. Carrier relaxation dynamics

Figure 2(a) shows the typical transient reflectivity changes (ΔR) of the 1D C_{60} polymer film obtained at $T = 40$, 100, and 270 K. The outline of the data is similar to those measured previously [22]. The sudden decrease in ΔR at $t \approx 0$ fs is caused by the electrons excitation by the pump pulse. The subsequent decay reflects their relaxation via e-ph scatterings, which will be characterized by its decay time below. There is also a slow decay component, where the oscillations of ΔR becomes dominant at delay time t longer than 10 ps. Such oscillations have often been observed in the pump-probe reflection measurements of the thin films [32] and are attributed to a result of the moving acoustic pulses generated by the instantaneous relaxation of electrons. Hereafter we neglect the oscillation component for evaluating the λ value directly from the nonequilibrium electrons relaxation. Based on the two kinds of decay components, fast and slow components, we extracted the associated relaxation time by fitting the measured reflectance with the following equation:

$$\Delta R \propto A_{\mathrm{fast}} \exp\left(-\frac{t}{\tau}\right) + C_{\mathrm{slow}}. \quad (1)$$

Here τ denotes the relaxation time corresponding to the fast component, whereas A_{fast} and C_{slow} are the amplitude of the fast and slow component, respectively. We assume the relaxation time of the slow component to be infinite because of its long decay time on the order of nanoseconds.

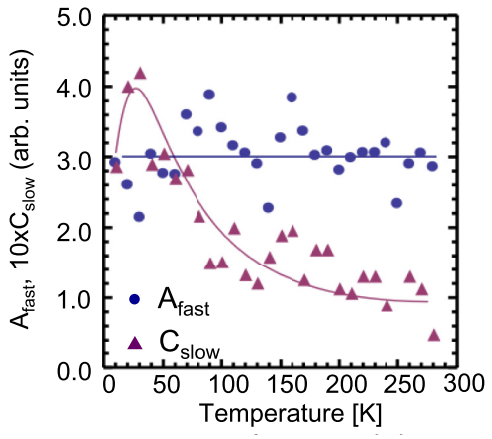

FIG. 3. (Color online) The amplitudes of both A_{fast} (solid circle) and C_{slow} (solid triangle) defined in Eq. (1) as a function of temperature. The solid curves are guides to the eyes.

To enhance the difference in ΔR among the temperatures [see Fig. 2(a)], we plot a curve (solid line at $T = 270$ K and dashed lines at $T = 40$ and 100 K) obtained by a fit to the data at $T = 270$ K using Eq. (1): the differences are indicated by the shaded areas. As T decreases, the decay time of τ became faster. To analyze the relaxation dynamics in more detail, we examined T dependence of τ, as shown in Fig. 2(b). At temperatures above 100 K, τ exhibited a quasilinear T dependence, which implies that the relaxation dynamics is governed by the e-ph interaction. According to the equation derived by Kabanov and Alexandrov [33], the τ caused by the e-ph interaction in a metal can be expressed by the following relationship:

$$\tau = \frac{2\pi k_B T}{3\hbar\lambda\langle\omega^2\rangle}. \tag{2}$$

Here k_B is the Boltzmann constant, ω is the phonon frequency, and $\hbar$ is the reduced Planck's constant. In addition, $\lambda\langle\omega^n\rangle = 2\int_0^\infty \alpha^2F(\omega')(\omega')^{n-1}d\omega'$, where $\alpha^2F(\omega)$ is the Eliashberg function. Since the relaxation time at $T > 100$ K is larger than the pulse width ~120 fs, it is reasonable to ignore the effect of the pulse width on the relaxation time. Using Eq. (2), we obtained $\lambda\langle(\hbar\omega)^2\rangle = 100$ (meV)^2. The magnitude of λ is discussed later. We next examine the slow component to complete the temperature dependent analysis.

Figure 3 shows the T dependence of both A_{fast} (solid circle) and C_{slow} (solid triangle) components. As T decreases from room temperature, C_{slow} increases gradually until ~80 K and drastically increases at temperatures below 80 K, while A_{fast} fluctuates and seems to be independent of T. The T dependence of the slow component suggests another relaxation process that dominates the carrier relaxation at temperatures below 80 K. We have previously reported that a phonon bottleneck mechanism considering the CDW gap formation dominates the carrier relaxation of the 1D C_{60} polymer film at temperatures below 50 K [22,23]. In the experiments, a similar temperature dependence of the amplitudes has been observed: The amplitude of the slow component increases as T decreases, while that of the fast one is independent of T [22]. It is reasonable to consider that the T dependence of C_{slow} obtained in the present study was due to the same mechanism.

B. Estimation of λ

To evaluate the magnitude of λ for the 1D C_{60} polymer, we assume that the Eliashberg function has the phonon density-of-states (DOS) shape, as assumed in Ref. [34]. Prior to estimating the upper limit of λ, we consider the following shape of DOS:

$$F(\omega) = A\left(\frac{\omega}{\omega_D}\right)^2\theta(\omega_D - \omega) + B\delta(\omega - \omega_E), \tag{3}$$

where ω_D is the cutoff frequency of acoustic phonon modes, and ω_E is the typical optical phonon frequency. $\theta(\omega)$ is the Heaviside step function. Normalization condition $\int_0^\infty F(\omega)d\omega = 1$ gives $A = 3(1-B)/\omega_D$. λ is a decreasing function of B in the present model. To estimate the upper limit of λ, we first consider the case of $B = 0$, i.e., only the interaction between electrons and acoustic phonons contributes to the magnitude of λ. Then we obtained $\lambda\langle(\hbar\omega)^2\rangle/\lambda = (\hbar\omega_D)^2/2 \simeq 1.0 \times 10^3$ (meV)^2 when we set $\hbar\omega_D = 45$ meV [23,35]. Thus we evaluated the magnitude of λ to be 0.1, which is comparable to that for AC_{60}. We next consider how the presence of the optical phonons lowers the magnitude of λ. We previously reported that the optical phonon mode with energy $\hbar\omega_E = 1340$ cm^{-1} = 166 meV has a large e-ph coupling [36]. When we set $B = 0.5$ and 1, we obtain $\lambda\langle(\hbar\omega)^2\rangle/\lambda = 5.5 \times 10^3$ and 5.5×10^4 (meV)^2, respectively. Then these values provide $\lambda =$ 0.02 and 0.002, respectively. Here the latter is the lower limit of λ. Since both the acoustic and optical phonons contribute to the e-ph interaction, it is reasonable to determine that the value of λ is 0.02 [37], which supports our prediction that the 1D C_{60} polymer has an intermediate value of between AC_{60} crystals and CNTs on the basis of the shape dependence of λ.

IV. DISCUSSION

The transient reflectivity in the present sample can be nicely fitted by a single-exponential decay, which means that excited electrons decay by emitting their energy into a single thermal bath. In the estimation of the e-ph coupling, we assumed that the oscillation period for the Debye frequency and the optical phonon frequency is ~0.1 and ~0.03 ps, respectively. These periods are clearly shorter than the observed relaxation time shown in Fig. 2(b). Therefore, it is reasonable to consider a phonon bath as the corresponding thermal bath. In fact, the relaxation time is linearly proportional to T, which is consistent with the relaxation dominated by the e-ph interaction discussed in Ref. [33]. Furthermore, the interaction between polymers is very weak, which has been evidenced by IR spectroscopy [26]. This fact eliminates the effect of the electronic transfer between polymers on the carrier relaxation.

We can validate our estimation of λ quantitatively via the determination of the length of the 1D C_{60} polymer, using the theory of Devos and Lannoo [38]. They examined the e-ph couplings for molecular crystals systematically, using density-functional theory within the local-density approximation and reported that λ can be factorized into $\lambda = N(E_F)V$, where $N(E_F)$ is the electron DOS at the Fermi level (E_F) and V is the intramolecular e-ph coupling. They showed that the value of V is inversely proportional to the number of π electrons (N_π) of atoms involved in the π states of the molecule, and derived the relationship $V = 1800/N_\pi$ meV. For example,

TABLE I. Electron-phonon coupling constant λ of nanocarbon allotropes. The kind of chemical bonding between C_{60} is also shown.

C_{60} compound	λ	Bonding (C_{60}-C_{60})
A_3C_{60} (A = K, Rb)	0.6 (0.5)	van der Waals
Na_4C_{60}	0.3	Single C-C σ bond
AC_{60} (A = K, Rb)	∼0.1	2 + 2 cycloadditional bond
1D C_{60} polymer	0.02	Coalesced GSW bond
Single-walled CNT	0.006	–
Multiwalled CNT	5.4×10^{-4}	–

$V = 300$ meV for C_6H_6 and $V = 50$ meV for C_{60}, though a slight deviation of the relation in the C_{60} may be attributed to a curvature effect due to its spherical shape. Since the interaction between adjacent 1D C_{60} polymers are governed by the van der Waals interaction, the 1D C_{60} polymers can be regarded as a molecular crystal. It is reasonable to set $N(E_F) \simeq 10/\text{eV/spin}$, because $N(E_F)$ of the 1D C_{60} polymer is slightly smaller than that of A_3C_{60} [39]. Then we evaluate $V = \lambda/N(E_F)$ to be 2 meV, which gives a value of $N_\pi = 900$. Since there are 60π electrons per one C_{60}, the value of $N_\pi = 900$ suggests that the 1D C_{60} polymer may consist of 15 C_{60} molecules at short, on which a conducting electron can move without any scattering. In fact, the length of tube consisting of 15 C_{60} molecules is in coincidence with the mean hopping distance of 8–13 nm obtained for the 1D C_{60} polymer film [24]. This strongly supports our estimation of the λ value. From the relation $\lambda = 1800N(E_F)/N_\pi$, the longer polymer has the smaller e-ph coupling, which would be verified by using other samples prepared on such as mica substrates instead of CsI substrates [28].

The concept of chemical bonding may provide us a unified understanding of the shape effects on the magnitude of λ for nanocarbons. Table I summarizes the value of λ for various nanocarbon allotropes, along with the classification of chemical bonding between adjacent C_{60} molecules. Since the strength of the chemical bonding can be ordered as follows: van der Waals < single C-C σ bond < 2 + 2 cycloadditional bond (two C-C σ bonds) < coalesced GSW bond (not only more than two C-C σ bonds but also C-C π bonds) [see also Figs. 4(a)–4(d)], it can be said that a stronger chemical bonding gives rise to a larger N_π in association with an enhancement in the electron hopping probability between adjacent C_{60} molecules. This results in a small value of V and λ, as described above for the 1D C_{60} polymers. The single-walled (or multiwalled) CNT is one extreme case [Fig. 4(e)].

Although we did not consider any lattice model for the 1D C_{60} polymer in the present study, we have already employed several kinds of models for the 1D C_{60} polymers, using the GSW transformation [40]. It would be theoretically interesting to investigate the e-ph interaction matrix elements for the excited electrons in those models. If the matrix elements involving the optical and/or acoustic phonons are strong, the nature of the interaction may be attributed to polar and/or deformation coupling, respectively. Unfortunately, calculations both of the phonon spectra and of the e-ph coupling constant for all the models require a large amount of computational time, owing to a large number of carbon atoms in a unit cell. This is in progress.

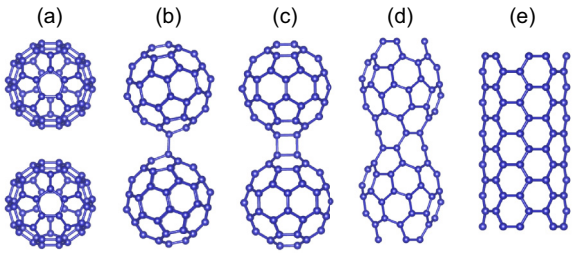

FIG. 4. (Color online) Schematic illustration of nanocarbon allotropes: two C_{60} between which are connected via (a) van der Waals interaction, (b) single C-C σ-bond, (c) 2 + 2 cycloadditional bond, (d) 1D C_{60} polymer having coalesced GSW bond, and (e) single-walled CNT.

Alternatively, electron transport measurements would be useful to investigate the nature of the e-ph interaction in low-dimensional systems. In fact, the e-ph interaction in the metallic CNTs has been studied using an atomic force microscope as an electrical probe [4]. A similar technique would enable us to clarify the nature of the e-ph interaction in the 1D C_{60} polymers, while we postulate that the nature of the interaction has an intermediate character between solid C_{60} and single-walled CNTs.

V. SUMMARY

In summary, we have examined carrier relaxation dynamics of the 1D C_{60} polymers, using femtosecond time-resolved pump-probe spectroscopy, and obtained the e-ph coupling constant (λ) to be 0.02, which supports our speculation that the 1D peanut-shaped C_{60} polymer has an intermediate value of between A_xC_{60} and CNTs on the basis of the shape of a π-electron conjugated system. This implies that the magnitude of an e-ph coupling constant for nanocarbon allotropes is significantly affected by the shape of a π-electron conjugated system. We believe that this finding becomes useful for a unified understanding of electron-phonon interaction for nanocarbon allotropes.

ACKNOWLEDGMENTS

We thank Professor K. Ohno, Mr. Y. Noda (Yokohama National University), and Dr. A. Takashima (Aoyama Gakuin University) for their helpful discussions. A part of the present work was financially supported by a Grant-in-Aid for Scientific Research on Innovative Areas (Grant No. 21200032) from the Ministry of Education, Culture, Sports, and Technology (MEXT).

[1] M. Kociak, A. Y. Kasumov, S. Guéron, B. Reulet, I. I. Khodos, Y. B. Gorbatov, V. T. Volkov, L. Vaccarini, and H. Bouchiat, Phys. Rev. Lett. **86**, 2416 (2001).

[2] M. J. Rosseinsky, A. P. Ramirez, S. H. Glarum, D. W. Murphy, R. C. Haddon, A. F. Hebard, T. T. M. Palstra, A. R. Kortan, S. M. Zahurak, and A. V. Makhija, Phys. Rev. Lett. **66**, 2830 (1991).

[3] W. Chen, A. V. Andreev, A. M. Tsvelik, and D. Orgad, Phys. Rev. Lett. **101**, 246802 (2008).
[4] J. Y. Park, S. Rosenblatt, Y. Yaish, V. Sazonova, H. Üstünel, S. Braig, T. A. Arias, P. W. Brouwer, and P. L. McEuen, Nano Lett. **4**, 517 (2004).
[5] M. F. Limonov, Y. E. Kitaev, A. V. Chugreev, V. P. Smirnov, Y. S. Grushko, S. G. Kolesnik, and S. N. Kolesnik, Phys. Rev. B **57**, 7586 (1998).
[6] Y. Wu, J. Maultzsch, E. Knoesel, B. Chandra, M. Huang, M. Y. Sfeir, L. E. Brus, J. Hone, and T. F. Heinz, Phys. Rev. Lett. **99**, 027402 (2007).
[7] G. K. Horton and A. A. Maradudin, *Dynamical Properties of Solids* (North-Holland, Amsterdam, 1985).
[8] O. Gunnarsson, Rev. Mod. Phys. **69**, 575 (1997).
[9] P. Zhou, K. A. Wang, P. C. Eklund, G. Dresselhaus, and M. S. Dresselhaus, Phys. Rev. B **48**, 8412 (1993).
[10] H. Kuzmany, J. Winter, and B. Burger, Synth. Met. **85**, 1173 (1997).
[11] T. Wågberg and B. Sundqvist, Phys. Rev. B **65**, 155421 (2002).
[12] T. Hertel, R. Fasel, and G. Moos, Appl. Phys. A **75**, 449 (2002).
[13] I. Chatzakis, Appl. Phys. Lett. **103**, 043110 (2013).
[14] H. Ueno, S. Osawa, E. Osawa, and K. Takeuchi, Fullerene Sci. Technol. **6**, 319 (1998).
[15] L. Guan, K. Suenaga, T. Okazaki, Z. Shi, Z. Gu, and S. Iijima, J. Am. Chem. Soc. **129**, 8954 (2007).
[16] J. Onoe, T. Nakayama, M. Aono, and T. Hara, Appl. Phys. Lett. **82**, 595 (2003).
[17] A. Takashima, J. Onoe, and T. Nishii, J. Appl. Phys. **108**, 033514 (2010).
[18] Y. Noda and K. Ohno, Synth. Met. **161**, 1546 (2011).
[19] A. Takashima, T. Nishii, and J. Onoe, J. Phys. D: Appl. Phys. **45**, 485302 (2012).
[20] S. Han, M. Yoon, S. Berber, N. Park, E. Osawa, J. Ihm, and D. Tománek, Phys. Rev. B **70**, 113402 (2004).
[21] J. Onoe, T. Ito, H. Shima, H. Yoshioka, and S. Kimura, Europhys. Lett. **98**, 27001 (2012).
[22] Y. Toda, S. Ryuzaki, and J. Onoe, Appl. Phys. Lett. **92**, 094102 (2008).
[23] S. Ono, H. Shima, and Y. Toda, Phys. Rev. B **86**, 104512 (2012).
[24] S. Ryuzaki and J. Onoe, Appl. Phys. Lett. **104**, 113301 (2014).
[25] J. Onoe and K. Takeuchi, J. Phys. Chem. **99**, 16786 (1995).
[26] J. Onoe, A. Takashima, S. Ono, H. Shima, and T. Nishii, J. Phys: Condens. Matter **24**, 175405 (2012).
[27] We investigated the structure of electron-beam-irradiated single crystal (SC) C_{60} film on mica using high-resolution transmission electron microscopy, as well as electron diffraction (ED), at room temperature. Comparison between experimental and simulated ED patterns demonstrates that a mixture of bco (body-centered orthorhombic) and hcp (hexagonal close-packed)-monoclinic based 1D peanut-shaped C_{60} polymer models well reproduces the experimental ED results of the EB-irradiated C_{60} SC film, where the distance between the C_{60} polymers is 0.928 nm [28]. In addition, we obtained the same IR spectra attributed to the 1D C_{60} polymer between mica and CsI substrates.
[28] H. Masuda, J. Onoe, and H. Yasuda, Carbon (2014).
[29] A. Takashima and J. Onoe (unpublished).
[30] J. Onoe, T. Ito, and S. Kimura, J. Appl. Phys. **104**, 103706 (2008).
[31] P. B. Allen, Phys. Rev. Lett. **59**, 1460 (1987).
[32] C. Thomsen, J. Strait, Z. Vardeny, H. J. Maris, and J. Tauc, and J. J. Hauser, Phys. Rev. Lett. **53**, 989 (1984).
[33] V. V. Kabanov and A. S. Alexandrov, Phys. Rev. B **78**, 174514 (2008).
[34] L. Stojchevska, P. Kusar, T. Mertelj, V. V. Kabanov, X. Lin, G. H. Cao, Z. A. Xu, and D. Mihailovic, Phys. Rev. B **82**, 012505 (2010).
[35] S. Ono and H. Shima, J. Phys. Soc. Jpn. **80**, 064704 (2011).
[36] J. Onoe, A. Takashima, and Y. Toda, Appl. Phys. Lett. **97**, 241911 (2010).
[37] This is a mean value of the e-ph interaction strength because the magnitude of the λ is given as an integration of the Eliashberg function that includes the e-ph interaction matrix elements, with respect to the phonon frequency. The detailed information of the different matrix elements will be averaged out and lost when the integration is performed.
[38] A. Devos and M. Lannoo, Phys. Rev. B **58**, 8236 (1998).
[39] G. Wang, Y. Li, and Y. Huang, J. Phys. Chem. B **109**, 10957 (2005).
[40] Y. Noda, S. Ono, and K. Ohno, Phys. Chem. Chem. Phys. **16**, 7102 (2014).